

# $\Lambda(1520)$ production in Z decays; Inclusive $\rho^0$ , $f_0(980)$ , $f_2(1270)$ , $K_2^{*0}(1430)$ and $f_2'(1525)$ Production in Z decays

DELPHI Collaboration

E. Schyns\*, Ch. Weiser  
*CERN, Switzerland*  
(\* corresponding author)  
(Emile.Schyns@cern.ch)

K. Hamacher, F. Seemann  
*Wuppertal University, Germany*

P. Chliapnikov, V. Ouvarov  
*IHEP Protvino, Russia*

Preliminary DELPHI results from two analyses are presented: 1.  $\Lambda(1520)$  production in  $Z^0 \rightarrow q\bar{q}$ , 2. Inclusive  $\rho^0$ ,  $f_0(980)$ ,  $f_2(1270)$ ,  $K_2^{*0}(1430)$  and  $f_2'(1525)$  production in  $Z^0 \rightarrow q\bar{q}$ . Both analyses are based on about 2 million multihadronic events collected in 1994 and 1995, using the particle identification capabilities of the DELPHI Ring Imaging Cherenkov detectors and measured ionisation losses in the Time Projection Chamber. The total production rates per hadronic Z decay have been determined to be:  $0.030 \pm 0.006$  for  $\Lambda(1520)$ ,  $1.19 \pm 0.10$  for  $\rho^0$ ,  $0.164 \pm 0.021$  for  $f_0(980)$ ,  $0.214 \pm 0.032$  for  $f_2(1270)$ ,  $0.073 \pm 0.023$  for  $K_2^{*0}(1430)$  and  $0.012 \pm 0.006$  for  $f_2'(1525)$ . The production rates and differential cross-sections are compared with the results of other LEP experiments and with model expectations. The mass dependence of meson production is investigated quantitatively whereas the origin of  $\Lambda(1520)$  production is investigated qualitatively.

## I. INTRODUCTION

At LEP it has been observed that a large fraction of primary produced particles in hadronic Z decays are of the orbitally excited state  $L=1$ . Results obtained on the production of orbitally excited particles are usually compared with the Lund string or cluster models [1,2] which are implemented in QCD-based Monte Carlo generators such as JETSET [3] and HERWIG [4]. For most particles, a reasonable description of the experimental data can be obtained after careful tuning of a number of adjustable parameters [5]. In this way, useful information can be acquired about the nature of the fragmentation process. However, for certain particles a significant disagreement with these models has been observed [6]. This is due to the fact that the physics of hadronization is not completely understood and the currently existing models cannot give sufficient guidance on possible differences in the production mechanisms of different mesons and baryons and on their dependences on spin and orbital momentum dynamics. In this view, studies of the production properties of the orbitally excited states are of particular interest.

This paper gives a short overview of two recent DELPHI analyses, the measurement of the orbitally excited ( $L=1$ )  $\Lambda(1520)$  baryon [7] and the measurement of likewise excited mesons  $\rho^0$ ,  $f_0(980)$ ,  $f_2(1270)$ ,  $K_2^{*0}(1430)$  and  $f_2'(1525)$ . More attention will be given to first analysis since the latter has been published elsewhere recently [8]. The analyses are based on about 2 million hadronic Z decays recorded by DELPHI during 1994 and 1995 LEP runs. Both analyses apply a standard track and hadronic event selection criteria and use the same  $\pi^\pm$ ,  $K^\pm$ , p and/or  $\bar{p}$  tagging technique as applied earlier in [9], i.e. combining the particle identification capabilities of the DELPHI Time Projection Chamber (TPC) and Ring Imaging Cherenkov (RICH) detectors and as such covering the full momentum range up to 45 GeV/c.

## II. $\Lambda(1520)$ PRODUCTION IN Z DECAYS

Apart from the above mentioned standard selection criteria, for the reconstruction of  $\Lambda(1520) \rightarrow pK$  only tracks in the DELPHI barrel region were selected ( $|\cos(\theta_{\text{track}})| < 0.68$ ). ‘Tight’ tagging was required for both particles and Outer Detector information was required for veto tracks, i.e. tracks giving no light in the RICH gas radiator.

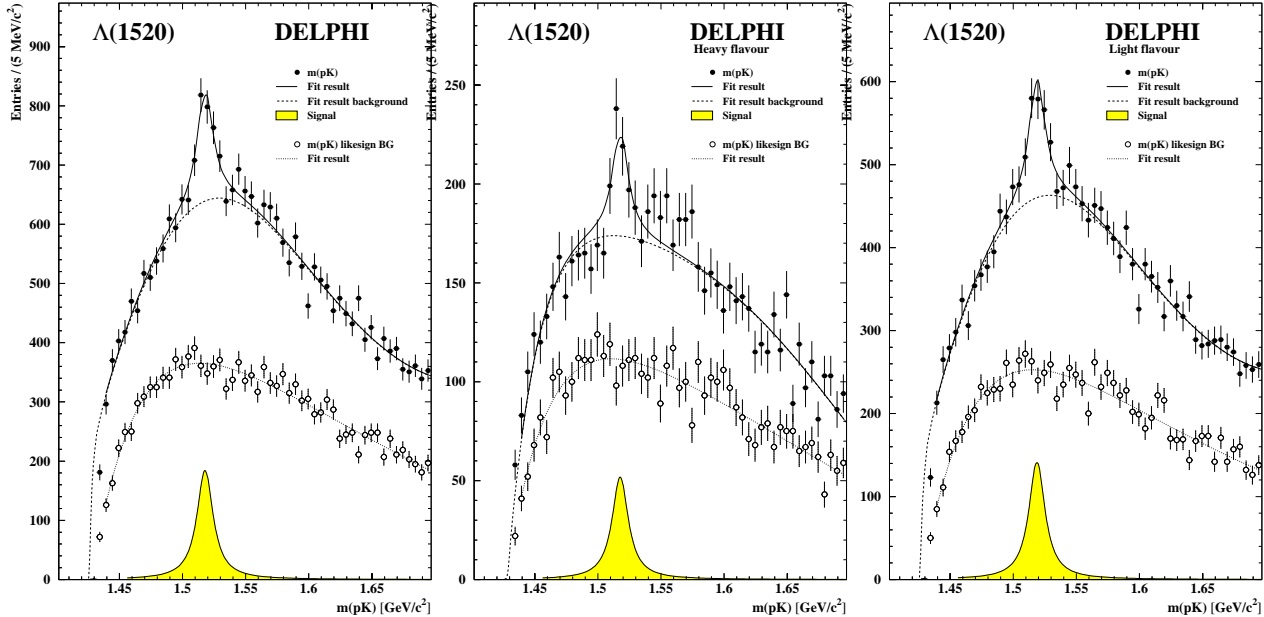


FIG. 1. The  $m(pK)$  invariant mass distribution for  $pK$  in  $Z^0 \rightarrow q\bar{q}$ . FIG. 2. The  $m(pK)$  distribution for heavy flavour enriched events. FIG. 3. The  $m(pK)$  distribution for light flavour enriched events.

In addition, the proton was required to have the largest of the two momenta and for both tracks the impact parameters were required to be less than 0.5 mm in  $R_\phi$  and less than 1 mm in  $z$ . Figure 1 shows the resulting  $pK$  invariant mass distribution (closed points) and the like-sign background (open points). The solid line represents a Breit-Wigner fit assuming a smooth background (dashed line). The signal after subtraction of background contains  $790 \pm 97$  candidates, shown on the bottom axis. To investigate whether the origin of the  $\Lambda(1520)$  depends on the primary quark flavour of the event, two subsamples were selected by applying a topological  $b$ -tag [7,9]. These were heavy primary flavour and light primary flavour enriched event samples of respectively  $\sim 70\%$   $bc$  purity ( $b$ -tag < 3%) and  $\sim 78\%$   $uds$  purity ( $b$ -tag > 3%). Equivalent to Figure 1, Figures 2 and 3 show the resulting  $pK$  invariant mass distributions, containing  $221 \pm 50$  and  $606 \pm 80$  candidates respectively. If the  $\Lambda(1520)$  originated solely from  $b$ - or  $c$ -decays, a much clearer signal should have appeared in Figure 2 and no signal in Figure 3. Conversely, if the  $\Lambda(1520)$  originated from fragmentation, most of the total signal should appear in Figure 3. This appears to be the case, and is supported by Figure 4 where no signal appears in the  $pK$  invariant mass distribution of identified Kaons and protons which do not originate from the interaction point and have been rejected by the impact parameter selection criteria. The differential cross-section as a function of the scaled energy  $X_E$  is shown in Figure 5, compared to OPAL data [10] and HERWIG [4]. Detector simulation based on 10000 JETSET  $\Lambda(1520)$  Monte Carlo events was used for corrections on the detec-

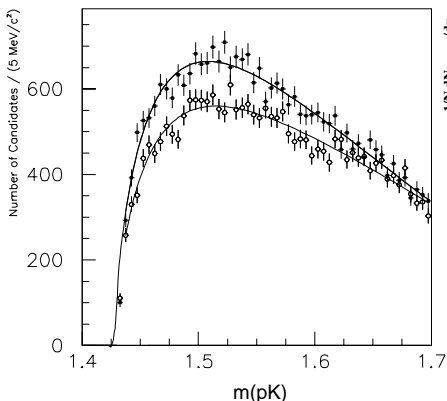


FIG. 4. The  $m(Kp)$  [ $\text{GeV}/c^2$ ] distribution (closed points) for identified protons and Kaons which have been rejected by the impact parameter selection criteria (the open points indicate the like-sign background).

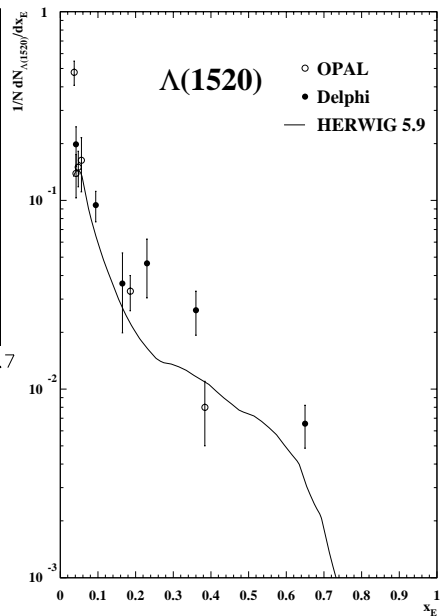


FIG. 5. The preliminary DELPHI  $\Lambda(1520)$   $X_E$  distribution vs OPAL and HERWIG.

tor acceptance, track reconstruction efficiency and particle identification efficiencies. No significant influences of reflections due to particle misidentification were found. The full  $X_E$  window was split into 6 intervals. By integrating the  $X_E$  distribution the inclusive  $\Lambda(1520)$  production rate was  $0.030 \pm 0.004$  (stat.)  $\pm 0.004$  (syst.) per hadronic Z decay. This result is compatible with the rate of  $0.0213 \pm 0.0021$  (stat.)  $\pm 0.0019$  (syst.) obtained by OPAL, but for  $X_E > 0.25$  the distribution seems to be harder than that from OPAL (not covering the full  $X_E$ -range).

### III. INCLUSIVE $\rho^0$ , $F_0(980)$ , $F_2(1270)$ , $K_2^{*0}(1430)$ AND $F_2'(1525)$ PRODUCTION IN Z DECAYS

This analysis has recently been published [8] and only some key points and final results will be discussed here. Tight selection criteria were required to achieve the highest possible purities of identified particles for the different resonances. Good agreement between the data and about 3 million detector simulated hadronic Z decays was observed. The window for the scaled momentum  $X_p$  was split in a maximum 7 intervals. The applied fit function for the different invariant mass distributions consists of three parts, covering signal, background and reflections. Systematic uncertainties were studied in great detail and an elaborate procedure was followed to account for reflections due to particle misidentification. Figure 6 shows the final  $X_p$  distributions obtained for  $\rho^0$ ,  $f_0(980)$  and  $f_2(1270)$ , compared to a previous DELPHI analysis and to available data from ALEPH [11], OPAL [12] as well as the JETSET prediction. The previous DELPHI analysis was based on less statistics and did not apply particle identification.

By integration of the  $X_p$  spectra, the total production rates per hadronic Z decay were found to be:  $1.19 \pm 0.10$  for  $\rho^0$ ,  $0.164 \pm 0.021$  for  $f_0(980)$ ,  $0.214 \pm 0.032$  for  $f_2(1270)$ ,  $0.073 \pm 0.023$  for  $K_2^{*0}(1430)$  and  $0.012 \pm 0.006$  for  $f_2'(1525)$ . The uncertainty is the quadratic sum of the systematic uncertainty and the uncertainty derived from the fits. The previous DELPHI analysis was based on less statistics and did not apply particle identification.

The DELPHI result on the total  $\rho^0$  rate agrees within the uncertainties with the value of  $1.45 \pm 0.21$  measured by ALEPH. The  $X_p$  spectra measured by the two experiments are also consistent with each other, although the  $X_p$  spectrum measured by ALEPH appears to be slightly harder at large  $X_p$  values than that measured by DELPHI. The total  $f_0(980)$  and  $f_2(1270)$  rates can be compared with the OPAL values of  $0.141 \pm 0.013$  and  $0.155 \pm 0.021$  respectively. The DELPHI and OPAL results on the  $f_0(980)$  total rate agree quite well. This is also true for the  $f_0(980)$   $X_p$  spectra. However, the  $f_2(1270)$   $X_p$  spectra measured by DELPHI and OPAL agree in shape but differ in the absolute normalisation, reflecting the difference in the respective total rates of 1.3 standard deviations.

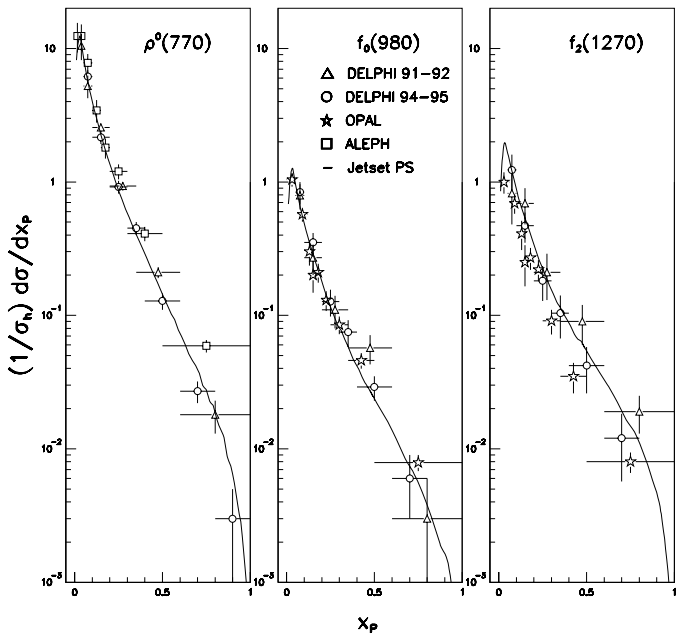


FIG. 6. The differential cross-sections for  $\rho^0$  (left),  $f_0(980)$  (middle) and  $f_2(1270)$  (right), compared to a previous DELPHI analysis (triangles) and to data from ALEPH [11] (squares), OPAL [12] (stars) and the JETSET prediction (full line).

### IV. RELATIVE RATES AND DISCUSSION

The agreement of the spectra in Figure 6 with the JETSET prediction is very satisfactory. The shapes of the  $\rho^0$ ,  $f_0(980)$  and  $f_2(1270)$   $X_p$  spectra for  $X_p \leq 0.4$  appear to be approximately the same. For  $X_p > 0.4$ , there is some indication that the  $f_0(980)$  and especially the  $f_2(1270)$   $X_p$  spectra are harder than the  $\rho^0$   $X_p$  spectrum. This is seen from Figure 7, where the ratios  $f_0(980)/\rho^0$  and  $f_2(1270)/\rho^0$  are shown as a function of  $X_p$ . The observed

increase of these ratios with increasing  $X_p$  is consistent with the JETSET expectations. Figure 8 shows the ratio of  $\Lambda(1520)/\Lambda(1115)$  as a function of  $X_p$ , compared to the HERWIG prediction. The  $\Lambda(1115)$  were taken from an ALEPH measurement [14]. Compared to the ratio of the  $f_2(1270)$  and  $\rho^0$  mesons shown in the previous figure, this distribution for baryons shows a similar shape and also here there is an indication that the  $\Lambda(1520)$  spectrum is harder than the  $\Lambda(1115)$  spectrum. The HERWIG prediction appears to be less hard compared to the data.

The total  $\rho^0$  rate can also be compared with the rate  $2.40 \pm 0.43$  of their isospin partners  $\rho^\pm$  recently measured by OPAL [13]. The ratio of the rates,  $2\rho^0/\rho^\pm = 0.99 \pm 0.20$ , is close to unity, as expected.

## DELPHI

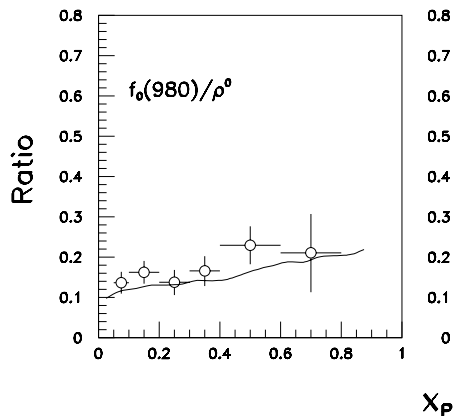


FIG. 7. The ratios of  $f_0(980)/\rho^0$  and  $f_2(1270)/\rho^0$  versus  $X_p$  compared to the JETSET prediction.

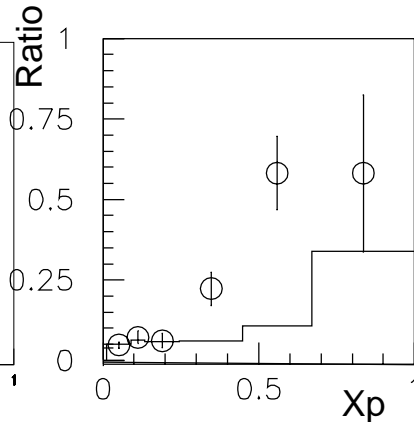


FIG. 8. The ratio of  $\Lambda(1520)/\Lambda(1115)$  versus  $X_p$  compared to the HERWIG prediction.

It is interesting to compare the total production rates of the tensor mesons  $f_2(1270)$ ,  $K_2^{*0}(1430)$  and  $f_2'(1525)$  with the respective rates of the vector mesons  $\rho^0$ ,  $K^{*0}(892)$  and  $\phi$ . Taking the  $K^{*0}(892)$  and  $\phi$  total rates from [6]:  $f_2(1270)/\rho^0 = 0.180 \pm 0.035$ ,  $K_2^{*0}(1430)/K^{*0}(892) = 0.095 \pm 0.034$  and  $f_2'(1525)/\phi = 0.115 \pm 0.058$ . The  $K_2^{*0}(1430)/K^{*0}(892)$  and  $f_2'(1525)/\phi$  ratios are similar within large errors, but smaller than the  $f_2(1270)/\rho^0$  ratio by 1.7 and 1.0 standard deviations respectively. Although the observed differences between the  $K_2^{*0}(1430)/K^{*0}(892)$ ,  $f_2'(1525)/\phi$  and  $f_2(1270)/\rho^0$  ratios are not very significant, they might indicate, that this is a simple consequence of the difference in particle masses and the mass dependence of the production rates.

This suggestion is supported by Figure 9, where the total rates,  $N(part)$ , measured by DELPHI for the  $\rho^0$ ,  $K^{*0}(892)$ ,  $f_0(980)$ ,  $\phi$ ,  $f_2(1270)$ ,  $K_2^{*0}(1430)$  and  $f_2'(1525)$  are plotted as a function of their mass squared,  $M^2$ . Anti-particles are not included in the  $K^{*0}(892)$  and  $K_2^{*0}(1430)$  rates. Both the  $\rho^0$ ,  $K^{*0}(892)$ ,  $f_0(980)$  and  $\phi$  data points and the  $f_2(1270)$  and  $K_2^{*0}(1430)$  and  $f_2'(1525)$  data points are well described ( $\chi^2/ndf = 0.07/2$  and  $0.01/1$ ) by exponentials of the form  $Ae^{-BM^2}$  (dashed lines), with the respective slope parameters  $5.43 \pm 0.25$  and  $4.13 \pm 0.63$ . The slopes are consistent with each other within two standard deviations. It can be noted that the  $\omega$ ,  $\rho^\pm/2$ ,  $a_0^\pm(980)/2$  and  $\eta'$  production rates measured by other LEP experiments [12] are also consistent with the exponential describing the  $\rho^0$ ,  $K^{*0}(892)$ ,  $f_0(980)$  and  $\phi$  data points. It appears that the production rates of particles with similar masses, such as the  $\rho^0$  and  $\omega$  or the  $f_0(980)$ ,  $a_0^\pm(980)$  and  $\eta'$  are very similar.

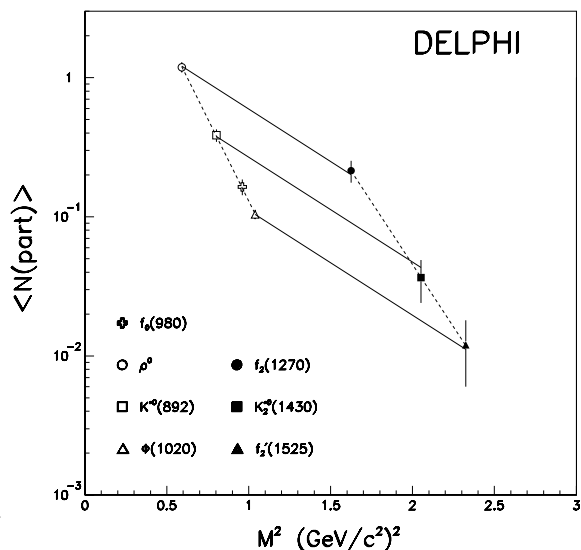


FIG. 9. The production rates of the vector and tensor mesons measured by DELPHI as a function of their mass squared (see text).

Figure 9 also shows that the mass dependence of the production rates is almost the same for the  $\rho^0$  and  $f_2(1270)$ ,  $K^{*0}(892)$  and  $K_2^{*0}(1430)$ ,  $\phi$  and  $f_2'(1525)$ . These three sets of data points are well fitted ( $\chi^2/ndf = 0.5/2$ ) to the exponential  $Ae^{-BM^2}$  (solid lines), with three different normalisation parameters  $A$  but the *same* slope parameter  $B$ , with a fitted value of  $1.74 \pm 0.15$ . Thus the relation between the production rates of tensor and vector mesons indeed appears to be very similar for different particles if the mass dependence of these production rates is taken into account.

## V. SUMMARY

Two recent DELPHI analyses have been shortly presented, the measurement of  $\Lambda(1520)$  production in hadronic Z decays and the measurement of  $\rho^0$ ,  $f_0(980)$ ,  $f_2(1270)$ ,  $K_2^{*0}(1430)$  and  $f_2'(1525)$  production in Z decays. Both analyses intensively used the particle identifying power of the DELPHI RICHes and TPC, to cover the full momentum window up to 45 GeV/c.

The spectrum of the  $\Lambda(1520)$  baryon versus the scaled energy was measured and appeared to be harder compared to OPAL data for  $X_E > 0.25$ . The production rate per hadronic Z decay was determined to be  $0.030 \pm 0.006$ . The  $\Lambda(1520)$  finding its origin in the fragmentation rather than in Z decays containing a heavy primary quark was investigated qualitatively. Also the distribution of the ratio  $\Lambda(1520)/\Lambda(1115)$  was determined and compared to the HERWIG prediction.

For the  $\rho^0$ ,  $f_0(980)$ ,  $f_2(1270)$ ,  $K_2^{*0}(1430)$  and  $f_2'(1525)$  the  $X_p$  spectra were measured and compared to the JETSET prediction. The production rates per hadronic event were determined to be  $1.19 \pm 0.10$  for  $\rho^0$ ,  $0.164 \pm 0.021$  for  $f_0(980)$ ,  $0.214 \pm 0.032$  for  $f_2(1270)$ ,  $0.073 \pm 0.023$  for  $K_2^{*0}(1430)$  and  $0.012 \pm 0.006$  for  $f_2'(1525)$ . Most of the spectra and production rates are found to be consistent with previous DELPHI data and also with ALEPH and OPAL data. The  $X_p$  dependence of  $f_0(980)/\rho^0$  and  $f_2(1270)/\rho^0$  was investigated as well as the dependence on the mass-squared of the production rates of vector and tensor mesons.

- [1] B. Andersson et al., Phys. Rep. **97** 31 (1993).
- [2] B.R. Webber, Nucl. Phys. **238** 492 (1984).
- [3] T. Sjöstrand, Comp. Phys. Comm. **82** 74 (1994).
- [4] G. Marchesini et al., Comp. Phys. Comm. **67** 465 (1992).
- [5] DELPHI Collab., P. Abreu et al., Z. Phys. **C73** 11 (1996).
- [6] DELPHI Collab., P. Abreu et al., Z. Phys. **C73** 61 (1996).
- [7] F. Seemann, Wuppertal University, Germany, Diploma Thesis, **WUD 98-28** (1999).
- [8] DELPHI Collab., P. Abreu et al., Phys. Lett. **B449** 364 (1999) and references therein.
- [9] DELPHI Collab., P. Abreu et al., E. Phys. J. **C5** 585 (1998) and references therein.
- [10] OPAL Collab., G. Alexander et al., Z. Phys. **C73** 569 (1997).
- [11] ALEPH Collab. D. Buskulic et al., Z. Phys **C69** 379 (1996).
- [12] OPAL Collab., R. Akerstaff et al., E. Phys. J. **C5** 411 (1998) and references therein.
- [13] OPAL Collab., R. Akerstaff et al., E. Phys. J. **C4** 19 (1998).
- [14] ALEPH Collab., G. Cowan et al., Phys. Rep. **294** 1 (1998).